High Efficiency Single Photon Detection via Frequency Up-Conversion

Aaron P. VanDevender and Paul G. Kwiat

Department of Physics, University of Illinois

1110 W Green St., Urbana, IL, USA

Abstract

We propose a method of single photon detection of infrared (IR) photons at potentially higher efficiencies and lower noise than allowed by traditional IR band Avalanche Photodiodes (APDs). By up-converting the photon from the IR, e.g., 1550 nm, to a visible wavelength in a nonlinear crystal, we can utilize the much higher efficiency of silicon APDs at these wavelengths. We have used a Periodically Poled Lithium Niobate (PPLN) crystal and a pulsed 1064-nm Nd:YAG laser to perform the up-conversion to a 631-nm photon. We observed conversion efficiencies as high as ~80%, and demonstrated scaling down to the single photon level while maintaining a background of 3×10^{-4} dark counts/count. We also propose a 2-crystal extension of this scheme, whereby orthogonal polarizations may be up-converted coherently, thus enabling complete quantum state transduction of arbitrary states.

1 INTRODUCTION

There are many applications which would benefit from the ability to detect single photons in the infrared. The physical characteristics of fiber optics lend themselves naturally to transmission at 1550 nm, and many telecommunications applications have gravitated to this wavelength. However, for applications which require fidelity at the single photon level, 1550-nm light has shown to be difficult to work with. Telecommunications systems where distance is limited by attenuation in fiber could extend their range by using detectors which are sensitive to single photons[1]. In quantum information applications such as quantum teleportation[2][3][4][5], quantum storage[6] and quantum cryptography[7][8][9], efficient detection of single photons is critical, since detector efficiency directly relates to the distance over which one can securely send messages[10][11][12]. Other uses of IR photon counters include infrared astronomy[13][14][15] and detection of single molecules[16][17] that have transitions in the infrared.

Until now, the best means of detecting these photons has been with infrared-optimized APDs, usually InGaAs or Ge. However, these detectors suffer from relatively low quantum efficiency, high dark counts and the need for cryogenic cooling. Recent implementations of the BB84 key distribution protocol[18] using a 1550-nm source found the optimal efficiency of the InGaAs detector to be only 11%[19]. While detector efficiencies up to 20% are attainable[20][21], the concomitant extra dark count noise reduces the final key generation rate. Hence, the efficiency limits the bit rate and distance achievable by the key distribution protocol, so any improvements over standard IR APDs would be beneficial for this type of application.

The nonlinear process of frequency up-conversion[22] can enable superior detectors of IR photons: By up-converting an infrared photon to a visible one, we can use silicon APDs which have much lower noise and higher efficiency for visible wavelengths. We are also developing a method of quantum state transduction whereby a single photon of one frequency in an *arbitrary* polarization state can be faithfully up-converted to a higher frequency while preserving the original polarization state. Such a capability is highly desirable, e.g., for distributed quantum computing. The transmission of qubits between quantum computers, especially over large distances, would most easily be accomplished by photons at 1550 nm (which has the highest transmission through fiber optics). However, depending on the scheme used for computation, the storage or processing of qubits may likely require photons in the visible spectrum, e.g., corresponding to some atomic transition, and so a method must be developed for converting between wavelengths at the single photon level while coherently maintaining the polarization state[23].

2 Frequency Up-Conversion

To achieve high efficiency frequency up-conversion, we utilize an intense escort laser pulse, a very weak input laser, and a bulk crystal of Periodically Poled Lithium Niobate (PPLN), quasi-phase-matched to the frequencies of the initial and escort photons. The resulting system up-converts one photon from the input beam and one photon from the escort beam into a single output photon. Due to energy conservation, the output frequency ω_o is the sum of the input frequency ω_i and the escort frequency ω_e. The relations that describe the nonlinear field evolution in a periodically poled nonlinear medium were given by Myers *et al.*[24]:

$$\frac{dE_i}{dz} = i\frac{\omega_i d_Q}{n_i c} E_o E_e^* \exp(i\Delta k_Q z) \tag{1}$$

$$\frac{dE_e}{dz} = i\frac{\omega_e d_Q}{n_e c} E_o E_i^* \exp(i\Delta k_Q z) \tag{2}$$

$$\frac{dE_o}{dz} = i\frac{\omega_o d_Q}{n_o c} E_i E_e \exp(-i\Delta k_Q z), \tag{3}$$

where E_i, E_e, and E_o are the electric field strengths of the input, escort, and output beams, respectively; n_i, n_e, and n_o are the indices of refraction at the three frequencies; d_Q is the effective nonlinear coefficient; and z is the longitudinal position within the crystal. Δk_Q describes the phase mismatch, here assumed to be zero (i.e., perfect phase-matching).

Because we will operate in the non-depletion regime ($E_i \ll E_e$), where the escort beam is not significantly depleted from up-conversion of the input beam, we can approximate $dE_e/dz \approx 0$. Eqs. (1)-(3) then reduce to two coupled first-order differential equations. Solving for E_o under the initial condition $E_0(z=0)=0$, we find a sinusoidal oscillation for the output field amplitude, which we can then convert to a probability of up-conversion $P_o(z)$:

$$P_o(z) \propto \sin^2\left(A\sqrt{I_e}z\right), \tag{4}$$

where A is a constant. [figure 1 should be about here] This evolution is essentially analogous to a Rabi oscillation between the input and output states, which is mediated by the strength of the escort field. The spatial period L_c for this process is

$$L_c = \sqrt{\frac{\pi^2 n_i n_o c^2}{\omega_i \omega_o d_Q^2 |E_e|^2}}. \tag{5}$$

For a crystal of length L_c (where L_c implicitly depends on the escort intensity), the input light will be completely up-converted to the output frequency, and then down-converted back to the original input frequency before leaving the crystal. For a given crystal length L, by choosing the escort intensity to give $L_c = 2L$, we can achieve very high conversion efficiency from ω_i to ω_o, as shown in figure 1. Note that by varying the escort power, we can also prepare photons in arbitrary superpositions of the "input" and "output" frequencies.

Such non-degenerate states may be important in future quantum information applications[25].

2.1 Quasi-Phase-Matching in Periodically Poled Crystals

Maximizing the nonlinear coefficient is important since the length of crystal required to achieve conversion is inversely proportional to d_Q. We chose to utilize a periodically poled nonlinear crystal rather than a traditional bulk nonlinear crystal because the former allows one to achieve quasi-phase matching and thereby take advantage of larger elements in the nonlinear susceptibility tensor[26]. In any nonlinear process, both energy and momentum must be conserved, implying the following phase matching conditions:

$$\omega_o = \omega_i + \omega_e \tag{6}$$

$$n_o\omega_o = n_i\omega_i + n_e\omega_e. \tag{7}$$

Because all nonlinear crystals are also dispersive (i.e., $n = n(\omega)$), it is impossible to satisfy both conditions simultaneously if all three beams are polarized in the same direction. Traditional phase matching overcomes this obstacle by using crystals which not only have a nonlinear response, but are also birefringent. For example, by properly orienting the optic axis of the crystal and making either one or both of the input and escort beams have ordinary polarization, the output beam is polarized in the extraordinary direction. This is known as Type-I (ordinary + ordinary → extraordinary) or Type-II (ordinary + extraordinary → extraordinary) phase matching. One problem with such birefringent phase-matching is that nonlinear crystals generally only very weakly couple modes that are polarized perpendicular to each other, i.e., the second-order nonlinear coefficients which dictate these processes are very small. For example, for stoichiometric[1] $LiNbO_3$ the largest coefficient relevant to traditional phase-matching (Type-I or Type-II) is $d_{31} = -4.64$ pm/V[27]. In contrast, the d_{33} nonlinear coefficient, which regulates the coupling of three *extraordinarily* polarized modes, is typically much larger than the coefficients which govern Type-I and Type-II processes. For $LiNbO_3$ d_{33} can be as large as -40 pm/V, almost an order of magnitude higher than d_{31}[27].

In order to take advantage of this larger tensor element, we must have a way to satisfy momentum conservation when all the interacting fields are identically polarized. This can be understood by noting

[1] Stoichiometric $LiNbO_3$ refers to $LiNbO_3$ which has a molar ratio of Li/Nb=1.0, as compared to "congruent" $LiNbO_3$ which has a molar ratio of Li/Nb=0.946.

that in Equations 1-3, where Δk_Q is taken to be the parameter which describes the regular phase-matching condition, the sign of dE_o/dz changes every time z changes by $\pi/\Delta k_Q$. Consequently, any increase of E_o in the first $\pi/\Delta k_Q$ length of crystal is immediately canceled out by the second $\pi/\Delta k_Q$ length of crystal. In quasi-phase-matching, the crystal is "poled" to create periodic ferroelectric domains, which contribute to the momentum, thus adding an extra term to Equation 7. The process of periodically poling a crystal uses a photolithography technique to create a mask of evenly spaced regions (ideally spaced at $\pi/\Delta k_Q$) running perpendicular to the optic axis of the crystal. An intense electric field is then applied to the regions exposed by the mask[28]. The electric field flips the direction of the nonlinear susceptibility of the crystal, which has the effect of changing the sign of the nonlinear coefficient. Consequently, the sign of d_Q is changed every $\pi/\Delta k_Q$ length of crystal, thus canceling out the overall sign of dE_o/dz (figure 2). By properly selecting Λ, the poling period of the crystal, we can create a quasi-phase matching situation which allows us to take advantage of the larger d_{33} nonlinear coefficient. The phase-mismatch is then given by

$$\Delta k_Q \equiv k_o - k_i - k_e - \frac{2\pi}{\Lambda} = 0, \tag{8}$$

where k_i, k_e, and k_o are the wavenumbers of the three beams in the crystal (i.e., $k = \omega n(\omega)/c$).

[figure 2 should be about here]

3 Experiment

3.1 PPLN Crystal

We are using 15-mm and 45-mm long multi-grating PPLN crystals [HC Photonics] to perform up-conversion (figure 3). The crystal is housed in an oven which heats it to 95°C (stable to within 0.1°C); at this temperature the 11.4μm poling period satisfies the quasi-phase-matching condition for 1550 nm + 1064 nm → 631 nm. Once the photon has been up-converted, it must be separated from the escort pulse before detection. We use prisms which have been cut at the Brewster angle to separate with very low loss the single 631-nm photon from the $\sim 10^{13}$ 1064-nm photons in each pulse. In combination with an additional 10-nm wide (FWHM) interference filter (transmission = 70% at 631 nm), the prisms are also effective in filtering out the spurious 532-nm light which is created in the crystal from second harmonic generation of the escort beam.

After filtering, the up-conversion photon is detected using a silicon APD [Perkin Elmer SPCM-AQ 222], with a measured efficiency of $41 \pm 5\%$, and a dark count rate of 400 $s^{-}1$. [figure 3 should be about here]

3.2 Escort Laser

Because of the intense electric field required of the escort laser (on the order of a megavolt per meter) we employ a pulsed laser.[2] We use a Nd:YAG "Nanolaser" [JDS Uniphase #NP-05011-110], which provides high intensity pulses (6μJ over ~500 ps; see figure 4a) at 1064 nm, at an approximate repetition rate of 7.2 kHz. [figure 4a and 4b should be about here] For a crystal length of 15 mm, with poling period $\Lambda = 11.4\,\mu m$, and a 13-kW escort pulse, we use a numerical model based on Equations 1-3 and the measured profile of the escort laser (figure 4a) to calculate that the peak conversion efficiency of a 1550-nm photon to a 631-nm photon should be close to 100% (as indicated by the near unit conversion efficiency peaks in figures 4b and 6). Furthermore, as long as this process operates in the non-depletion regime where $E_i \ll E_e$, the relationship between input power and output power is strictly linear. This means we can scale down the input power to the single photon level (or less); moreover, the output photon statistics should match the input statistics, but at the higher frequency, as has been previously demonstrated[30].

3.3 High Intensity Measurements

We have measured this up-conversion process, and have verified that it is linear as a function of the input intensity. Figure 5 shows a graph of the output intensity measured using a silicon photodiode [Newport 818-SL] at various 1550-nm input powers from 50 μW to 1.3 mW. In this experiment the escort beam is pulsed while the input beam is continuous, creating an output beam which is also pulsed. The absolute conversion efficiency from input to output is thus very low, since most of the input light passes through the crystal in between escort pulses. From the escort intensity profile (figure 4a) and the pulse repetition rate (~7.2 kHz), we can estimate a conversion efficiency over the FWHM of the escort pulse of $80 \pm 15\%$.

[figure 5 should be about here]

[2] Another option, which is being pursued by Albota, *et. al.*, is to employ a high-finesse power buildup cavity for the escort laser[29]. This has the advantage that one does not need to synchronize the photon to be up-converted. The disadvantage is the added complexity to achieve low loss coupling of the 1550 nm photon into the actively stabilized cavity.

3.4 Single Photon Measurements

In addition to measuring the up-converted intensity for a classical input beam, we have also measured high efficiency up-conversion at the single photon level. By using a series of neutral density filters, we attenuate our 1550-nm source such that, on average, less than a single photon overlaps with each escort pulse. Note that while this attenuation produces a weak coherent state and not a single photon Fock state, if the coherent state is weak enough such that the mean photon number is less than 1, the state is effectively a superposition of the single photon state and the vacuum state (which cannot initiate the up-conversion process). By taking into account the Poissonian weights of the two states, we can extrapolate our ability to up-convert a true single photon state by measuring weak coherent states. While up-conversion of true single-photon states (e.g., from a spontaneous parametric down-conversion source[31][32] or a quantum dot source[33][34][35][36]) remains an interesting experimental goal, the immediate application of IR up-conversion at the single-photon level is likely to use attenuated coherent states, the traditional source for fiber quantum cryptography systems.

During single-photon operation, by counting 631-nm photons in a 1-ns coincidence window around the escort pulse, we estimate a conversion efficiency at the single-photon level of $80 \pm 15\%$, in agreement with our previous measurement. The detector is an EG&G SPCM-AQ 222 avalanche photodiode, with a quantum efficiency of $41\pm5\%$. The 15% uncertainty in the conversion efficiency is a product of the uncertainties in the detector efficiency, the intensity of the weak-coherent pulse (whose uncertainty in turn arises mainly from the difficulty in precisely calibrating the 12 orders of magnitude optical attenuation to produce the 1550-nm photons) and the intensity profile of the escort pulse. We estimate the efficiency based on the escort intensity by integrating the conversion efficiency profile (figure 4b) over the duration of the pulse, which gives the total "conversion time window" for the input beam. Multiplying the time window by the input photon rate yeilds the mean number of up-converted photons.

We have also measured the background, defined as the probability of a false count (detection event when no 1550-nm signal is present) occurring during a 1-ns window. We observed 3×10^{-4}, and anticipate that further design improvements could reduce this background by another order of magnitude. One source contributing to the background is down-conversion of the bright 1064-nm beam into a 1550-nm photon (and a 3393-nm photon), followed by subsequent up-conversion with the 1064-nm escort into a spurious 631-nm photon. Although phase-matching conditions for down-conversion from 1064 nm into 1550 nm and 3393 nm are far off resonance, there still exists some probability for this process to occur. In particular, if only one of the roughly 10^{13} 1064-nm photons in each pulse were to down-convert into 1550 nm + 3393 nm, our signal would be completely overwhelmed by the resulting background. This spurious down-conversion process is only one of the sources of background. The remainder of the background is due to detector dark counts, ambient background light and fluorescence from the 1064-nm pulse off optical surfaces. We have observed the fluorescence effect to have a peak at the time of the escort pulse, followed by a $\sim$100-ns decay. This allows much of the fluorescence background to be excluded by coincidence gating around the escort pulse arrival time. Determining the precise relative composition of these background sources, and techniques for reducing them, are subjects of future investigations.

4 Discussion

Since the conversion efficiency is a function of the intensity of the escort pulse, in order to maximize the up-conversion probability it is necessary to make the single photon wavepacket somewhat shorter than the escort pulse, such that in the region of overlap, the escort intensity looks relatively constant. The total conversion efficiency due to pulse overlap is given by

$$P_{overlap} = \int_{-\infty}^{+\infty} P_o(I_e(t)) I_i(t) dt, \tag{9}$$

where I_i is the normalized input pulse profile ($\int_{-\infty}^{+\infty} I_i(t)dt = 1$), and P_o is given in Equation 4. We are helped by the fact that the conversion efficiency's dependence on escort intensity I_e varies like $\sin^2(\sqrt{I_e})$ (figure 1). This function actually flattens out the conversion efficiency near the peak, as shown in figure 4b, and so it is not necessary for the single photon wave-packet to be drastically shorter than the escort pulse. In fact, because the spread in frequency (and hence momentum) is inversely proportional to wave packet duration (assuming a transform-limited pulse), if the duration is too short, it will not be possible to completely satisfy the conservation of momentum phase-matching condition (7), and the conversion efficiency will actually *decrease* (see Fig. 6). We must balance between making the escort pulse appear constant (short signal-pulse duration) and keeping the frequency spread to a minimum (long pulse duration) in order to achieve maximum conversion efficiency. For our system parameters we calculate an optimal pulse width of 100 ps, with a corresponding conversion efficiency of 99.4%; however, for all widths in the range 10 ps to 450 ps, the conversion efficiency is still predicted to be greater than 90%. One benefit of using a pulsed escort (as opposed to one that is always on, as, e.g., in [29]) is that one may rely on the fact that efficient up-conversion only occurs if the signal photon arrives within a very narrow time window. In this way one can realize a "gated" detector where time resolution is limited only by the escort pulse duration, and not the time resolution of the final physical detector used to detect the visible photon. [figure 6 should be about here]

5 State Transduction

The scheme described above operates on only one of the polarizations of the initial photon, since it must be extraordinary in the PPLN. However, in many quantum communication protocols, it may be desirable to faithfully convert an *arbitrary* state of polarization. For example, realization of quantum teleportation[3][4][5]—a necessary ingredient in creating quantum repeaters[37][38][39]—over long distances through fibers could require entangled photon transmission at 1550 nm, the maximum transmission wavelength for telecommunication fibers. However, the requisite Bell-state analysis is, at present, substantially more efficient and accurate using visible photon counters. As a second example, the coupling of distant quantum computers to form a quantum network could similarly require transmission of optical qubits at telecom wavelengths. However, the energies of these photons are unlikely to be commensurate with the transition energies of the non-optical quantum bits in the computing nodes. Therefore, frequency conversion of the telecom qubits to match the computing qubits will be necessary.

To faithfully convert an arbitrary polarization state we propose to employ a second PPLN crystal in series with the first, but oriented such that its optic axis is rotated by 90° around the propagation direction. By using an escort laser polarized at 45° (i.e., with equal horizontal and vertical components), we can up-convert the horizontal component of the input photon in the first crystal and the vertical component in the second, as shown in figure 7. [figure 7 should be about here] As long as the group-velocity dispersion effects do not lead to a time-labeling of the conversion processes (i.e., as long as the process of up-conversion in one crystal is *indistinguishable* from up-conversion in the other[3]) these two processes will occur *coherently*, and an arbitrary initial quantum state can be up-converted. Dispersion and birefringence effects in the PPLN crystal will cause the final up-converted photon to have an additional phase ϕ between its horizontal and vertical components. However, using an appropriate birefringent element to compensate for this phase, we believe we can prepare a high-frequency photon which has the same polarization state as the initial photon, with very high fidelity. Moreover, if the initial photon were *entangled* to another photon, the entanglement would be transfered to the higher frequency photon.

6 Conclusions

Infrared single photon detection through frequency up-conversion using periodically poled $LiNbO_3$ is shown to be a viable alternative to traditional InGaAs and Ge APDs, which suffer from high noise, low efficiency, and the need for cryogenic cooling. By poling the ferroelectric domains of a nonlinear crystal to satisfy the quasi-phase-matching conditions, we can efficiently convert a 1550-nm photon into a 631-nm photon, which can then be detected by a silicon APD[4]. Further avenues of research include attempting to convert an arbitrary polarization state using the 2-crystal scheme described above, and investigating the use of a waveguide structure to increase the conversion efficiency. In the latter case, the benefit could be a reduction in the required escort power by several orders of magnitude, due to the much smaller mode volume (implying a higher electric field for the same optical power)[46][47][48][49]. In particular, it was recently demonstrated that waveguides can be created in nonlinear crystals without disturbing the ferroelectric domain poling, using a soft proton-exchange method[28]. If sufficient gains on the conversion efficiency can be made, it may even be possible to employ a CW escort beam[29], which would enable up-conversion of photons arriving at arbitrary times.

[3]The reverse process—mapping the polarization state of a pump photon onto two correlated down-conversion photons—is now a standard method to prepare high fidelity polarization-entangled photon pairs[40]. See also the recent work on complete Bell state analysis by Kim, Kulik, and Shih[41]

[4]One option to further increase the net detection efficiency would be to detect the visible photon using solid state photomultipliers[42][43] or visible light photon counters[44][45]. These devices operate using impurity band to conduction band excitations, and may have single photon detection efficiencies in excess of 90%.

Acknowledgments

This work was supported by the MURI Center for Photonic Quantum Information Systems (ARO/ARDA program DAAD19-03-1-0199). Additional funding for this research was provided by the DCI postdoctoral program. We would like to thank Richard Hughes of Los Alamos National Laboratory and ARDA for their assistance in conducting this research, as well as thank Franco Wong and Marius Albota from MIT for helpful discussions.

References

[1] A. Karlsson *et al.* Single-photon counter for long-haul telecom. *IEEE Circuits and Devices Magazine*, 15:34–40, 1999.

[2] C. H. Bennett *et. al.* Teleporting an unknown quantum state via dual classical and einstein-podolsky-rosen channels. *Phys. Rev. Lett.*, 70:1895–9, 1993.

[3] D. Bouwmeester *et al.* Experimental quantum teleportation. *Nature*, 390:575–579, 1997.

[4] A. Furusawa *et al.* Unconditional quantum teleportation. *Science*, 282:706–9, 1998.

[5] P. K. Lam, W. P. Bowen, and T. C. Ralph. Quantum teleportation with Einstein-Podolsky-Rosen optical entanglement. *Physicist*, 39:72–77, 2002.

[6] T. B. Pittman and J. D. Franson. Cyclical quantum memory for photonic qubits. *Phys. Rev. A*, 66:62302–1–4, 2002.

[7] N. Gisin, G. Ribordy, W. Tittel, and H. Zbinden. Quantum cryptography. *Rev. Mod. Phys.*, 74:145, 2002.

[8] M. Bourennane *et al.* Experimental long wavelength quantum cryptography: From single-photon transmission to key extraction protocols. *J. Mod. Opt.*, 47:563–579, 2000.

[9] R. J. Hughes *et al.* Quantum cryptography for secure satellite communications. In *2000 IEEE Aerospace Conference*, volume 1 of *IEEE Aerosp. Conf. Proc.*, pages 191–200, 2000.

[10] S. N. Molotkov and S. S. Nazin. Is there a fundamental limit on the length of a communication channel in a single-photon quantum cryptosystem? *JETP Lett.*, 64:866–9, 1996.

[11] N. Lütkenhaus. Security against individual attacks for realistic quantum key distribution. *Phys. Rev. B.*, 61:052304, 2000.

[12] E. Waks, C. Santori, and Y. Yamamoto. Security aspects of quantum key distribution with sub-Poisson light. *Phys. Rev. A*, 66:042315, 2002.

[13] R. W. Boyd and C. H. Townes. An infrared upconverter for astronomical imaging. *Appl. Phys. Lett.*, 31:440, 1977.

[14] E. C. Cheung, K. Koch, and G. T. Moore. Frequency upconversion by phase-matched sum-frequency generation in an optical parametric oscillator. *Opt. Lett.*, 23:1967–1969, 1994.

[15] M. Poulain. Fluoride glass fibers: applications and prospects. In *Infrared Glass Optical Fibers and Their Applications*, volume 3416 of *Proc. SPIE*, pages 2–12, 1998.

[16] S. A. Soper. Single-molecule detection in the near-ir using continuous-wave diode laser excitation with an avalanche photon detector. *Appl. Spectroscopy*, 52:1–6, 1998.

[17] A. Castro and E. Brooks Shera. Single-molecule detection: applications to ultrasensitive biochemical analysis. *Appl. Optics*, 34:3218–22, 1995.

[18] C. H. Bennett and G. Brassard. Quantum cryptography: Public key distribution and coin tossing. In *Proceedings of IEEE International Conference on Computers, Systems and Signal Processing*, 1984.

[19] R. J. Hughes, G. L. Morgan, and C. G. Peterson. Quantum key distribution over a 48-km optical fiber network. *J. Modern Optics*, 47:533, 2000.

[20] M. Bourennane, A. Karlsson, J. P. Ciscar, and M. Mathés. Single-photon counters in the telecom wavelength region of 1550 nm for quantum information processing. *J. Modern Optics*, 48:1983–1995, 2001.

[21] D. Stucki *et al.* Photon counting for quantum key distribution with Peltier cooled InGaAs/InP APDs. *J. Modern Optics*, 48:1967–1981, 2001.

[22] A. Yariv. *Quantum Electronics*. Wiley, New York, 1988.

[23] J. Shapiro. Architectures for long-distance quantum teleportation. *New Journal of Physics*, 4:47.1–47.18, 2002.

[24] L. E. Myers *et al.* Quasi-phase-matched optical parametric oscillators in bulk periodically poled $LiNbO_3$. *J. Opt. Soc. Am. B*, 12:2102–2116, 1995.

[25] G. Giorgi, P. Mataloni, and F. De Martini. Frequency hopping in quantum interferometry: Efficient up-down conversion for qubits and ebits. *Phys. Rev. Lett.*, 90:027902, 2003.

[26] L. E. Myers and W. R. Bosenberg. Periodically poled lithium niobate and quasi-phase-matched optical parametric oscillators. *IEEE Journal of Quantum Electronics*, 33:1663–1672, 1997.

[27] V. G. Dmitriev, G. G. Gurzadyan, and D. N. Nikogosyan. *Handbook of Nonlinear Optical Crystals*. Springer-Verlag, Heidelberg, Germany, 1999.

[28] L. Chanvillard, P. Aschiéri, P. Baldi, D. B. Ostrowsky, M. de Micheli, L. Huang, and D. J. Bamford. Soft proton exchange on periodically poled $LiNbO_3$: A simple waveguide fabrication process for highly efficient nonlinear interactions. *App. Phys. Lett.*, 76:1089–1091, 2000.

[29] M. A. Albota and F. N. C. Wong. Efficient single-photon counting at 1.55 μm via frequency upconversion. In *Postdeadline Papers Book*, Conference on Lasers and Electro-Optics/Quantum Electronics & Lasers Science Coneference, 2003.

[30] J. Huang and P. Kumar. Observation of quantum frequency conversion. *Phys. Rev. Lett.*, 68:2153, 1992.

[31] T. B. Pittman, B. C. Jacobs, and J. D. Franson. Single photons on pseudodemand from stored parametric down-conversion. *Phys. Rev. A*, 66:042303/1–7, 2002.

[32] A. L. Migdall, D. Branning, and S. Castelletto. Tailoring single-photon and multiphoton probabilities of a single-photon on-demand source. *Phys. Rev. A*, 66:053805/1–4, 2002.

[33] P. Michler *et. al.* A quantum dot single-photon turnstile device. *Science*, 290:2282–5, 2000.

[34] C. Santori, M. Pelton, G. Solomon, Y. Dale, and Y. Yamamoto. Triggered single photons from a quantum dot. *Phys. Rev. Lett.*, 86:1502–5, 2001.

[35] Z Yuan *et al.* Electrically driven single-photon source. *Science*, 295:102–5, 2002.

[36] J. Kim, O. Benson, H. Kan, and Y. Yamamoto. A single-photon turnstile device. *Nature*, 397:500–3, 1999.

[37] H.-J. Briegel, W. Dür, J. I. Cirac, and P. Zoller. Quantum repeaters: The role of imperfect local operations in quantum communication. *Phys. Rev. Lett.*, 81:5932–5, 1998.

[38] A. M. Bychkov and D. Bouwmeester. Single-photon storage in a single quantum dot for the implementation of a solid-state quantum repeater. In *10th International Symposium on Nanostructures: Physics and Technology*, volume 5023 of *Proc. SPIE*, pages 572–573, 2003.

[39] Z. Zhao, T. Yang, Y. Chen, A. Zhang, and J. Pan. Experimental realization of entanglement concentration and a quantum repeater. *Phys. Rev. Lett.*, 90:207901/1–4, 2003.

[40] A. G. White, D. F. V. James, W. J. Munro, and P. G. Kwiat. Exploring Hilbert space: Accurate characterization of quantum information. *Phys. Rev. A*, 65:012301, 2002.

[41] Y. H. Kim, S. P. Kulik, and Y. Shih. Quantum teleportation of a polarization state with a complete Bell state measurement. *Phys. Rev. Lett.*, 86:1370, 2001.

[42] P. G. Kwiat *et al.* High efficiency single-photon detectors. *Phys. Rev. A*, 48:R867, 1993.

[43] P. H. Eberhard, P. G. Kwiat, M. D. Fetroff, M. G. Stapelbroek, and H. H. Hogue. Detection efficiency and dark pulse rate of rockwell (SSPM) single photon counters. In *Proceedings of the IEEE International Conference on Applications of Photonics Technology*, (ICAPT '94), June 22-24, 1994.

[44] J. Kim, S.Takeuchi, Y.Yamamoto, and H.H.Hogue. Multiphoton detection using visible light photon counter. *Appl. Phys. Lett.*, 74 (7):902–904, (February 1999).

[45] S.Takeuchi, J.Kim, Y.Yamamoto, and H.H.Hogue. Development of a high-quantum-efficiency single-photon counting system. *Appl. Phys. Lett.*, 74 (8):1063–1065, (February 1999).

[46] A. L. Campillo, J. W. P. Hsu, K. R. Parameswaran, and M. M. Fejer. Direct imaging of multimode interference in a channel waveguide. *Opt. Lett.*, 28:399–401, 2003.

[47] M. C. Booth *et al.* Counterpropagating entangled photons from a waveguide with periodic nonlinearity. *Phys Rev. A.*, 66:02381, 2002.

[48] K. Banaszek, A. B. U'Ren, and I. A. Walmsley. Generation of correlated photons in controlled spatial modes by downconversion in nonlinear waveguides. *Opt. Lett.*, 26:1367–1369, 2001.

[49] M. G. Roelofs, A. Suna, W. Bindloss, and J. D. Bierlein. Characterization of optical waveguides in $KTiOPO_4$ by second harmonic spectroscopy. *J. Appl. Phys.*, 76:4999–5006, 1994.

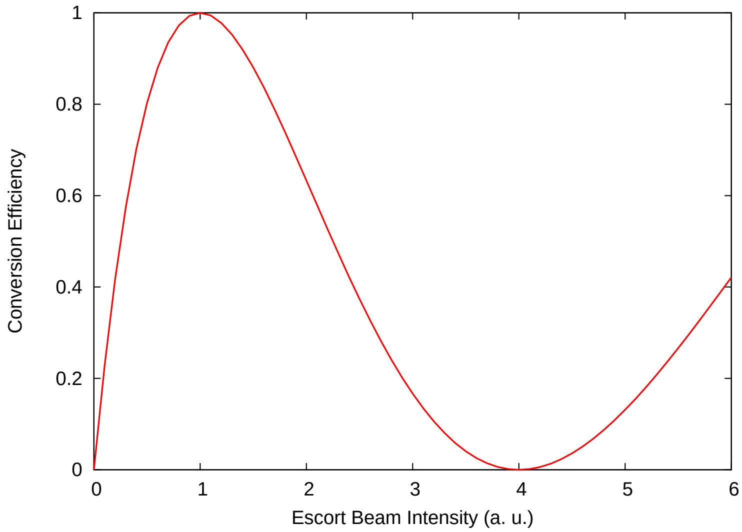

Figure 1: Up-conversion efficiency of a weak input beam versus the intensity of the escort light, as given by Equation 4.

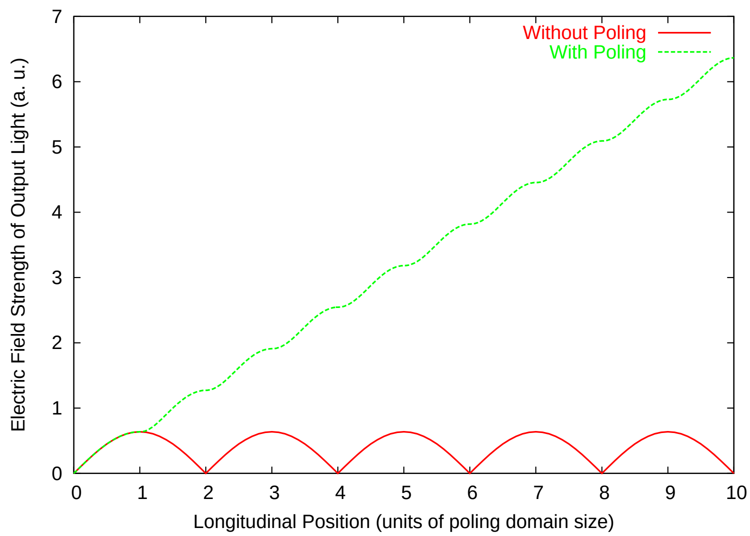

Figure 2: Electric field strength of output light versus longitudinal position, assuming *no* birefringent phase matching. For the case of no poling, the output field increases a small amount before the phase mismatch reaches π, at which point the output field decreases back to zero. This evolution is described by Equations 1,2, and 3 when $\Delta k_Q \neq 0$. These alternating regions of increasing and decreasing output field cancel each other out, yielding at best a very small net conversion probability. By reversing the ferroelectric domain every $\pi/\Delta k_Q$, thereby setting the effective Δk_Q for the poled system to 0, we achieve an initial steady growth in the output field, as long as the output field is much smaller than the input field. Since the typical period for complete conversion to the output field is on the order of thousands of poling domains, the evolution of the output field is well characterized by a sine function of the longitudinal position, i.e., we can ignore the small fluctuations illustrated in this figure and approximate the full up-conversion process for the poled system with Equation 4.

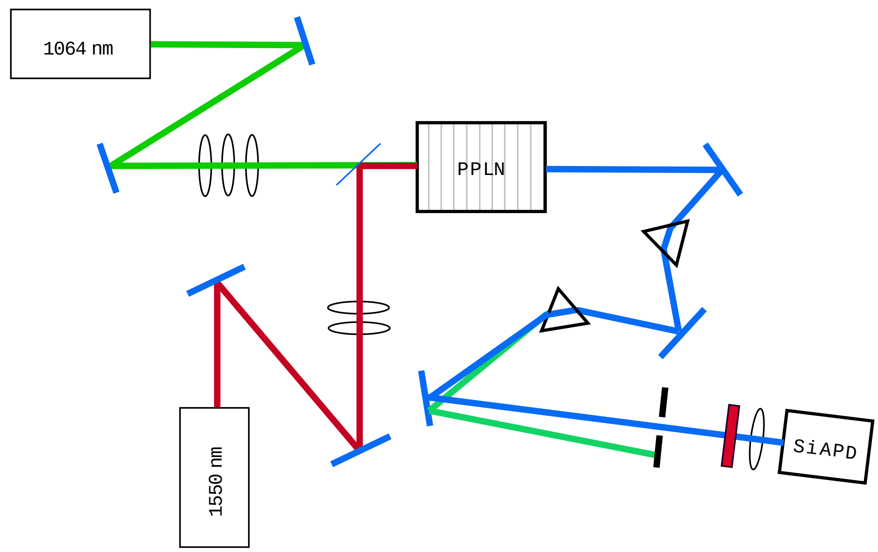

Figure 3: Scheme to efficiently convert an infrared initial photon to a visible wavelength final photon. An initial photon at 1550 nm and a 1064-nm escort pulse are sent into a sample of Periodically Poled Lithium Niobate (PPLN). For appropriate crystal and escort pulse parameters, there is a near-unity probability of up-converting to a 631-nm photon.

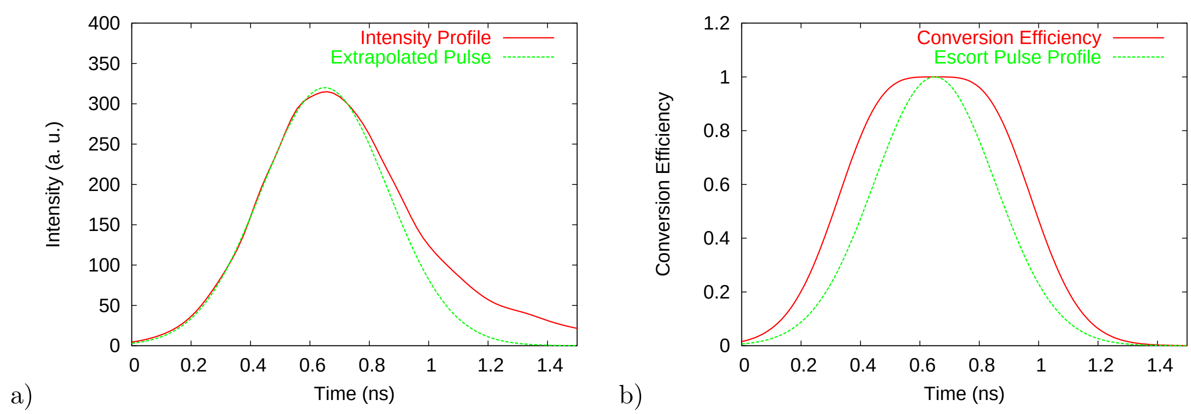

Figure 4: (a) Measured intensity profile for the 1064-nm escort laser (solid line) and the extrapolated Gaussian pulse profile (dotted line). We believe the measured intensity diverges from the Gaussian extrapolation at $\sim$1 ns because of limitations of the fall time of the detector [EOT ET-3500 10GHz InGaAs Photodiode]. (b) Predicted conversion efficiency (solid) using our extrapolated escort pulse profile (dotted). This is the result of applying Equation 4 to each point of the intensity profile.

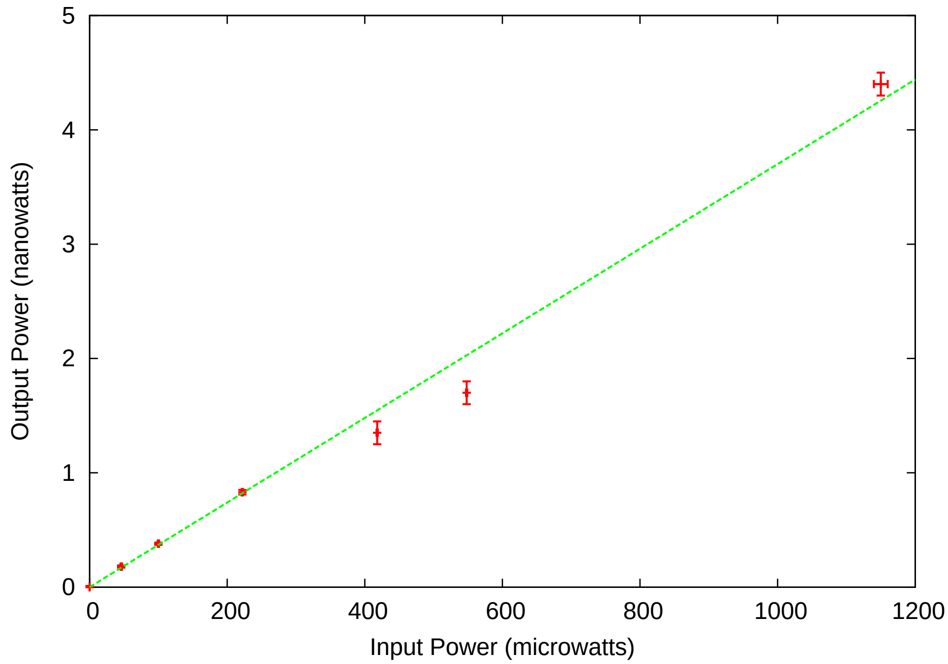

Figure 5: Output intensity of 631-nm light, as a function of input 1550-nm intensity. The dotted line is a linear fit to the data. Note that the implied efficiency is very low because the initial light was CW, i.e., most of the time there was no escort light.

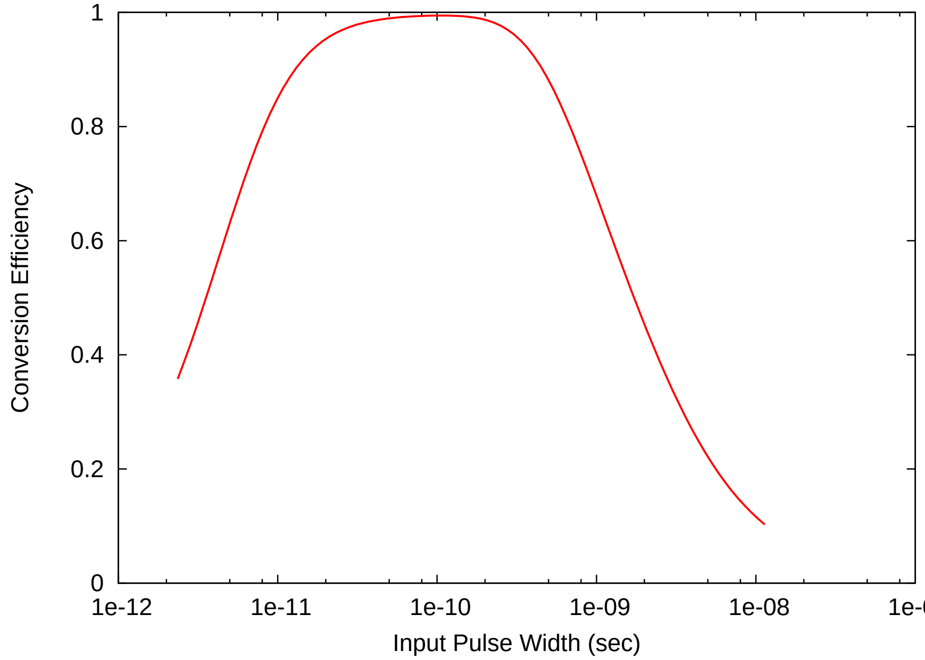

Figure 6: Conversion efficiency as a function of signal pulse width, assuming a Gaussian escort pulse with FWHM = 500 ps. The curve illustrates the trade-off between using signal pulses shorter than the escort pulse (to prevent averaging over different conversion probabilities) and minimizing the spread in frequency, and consequently in momentum (to satisfy the phase-matching condition). The peak theoretical conversion efficiency is 99.4% and occurs for an input pulse width of 100 ps.

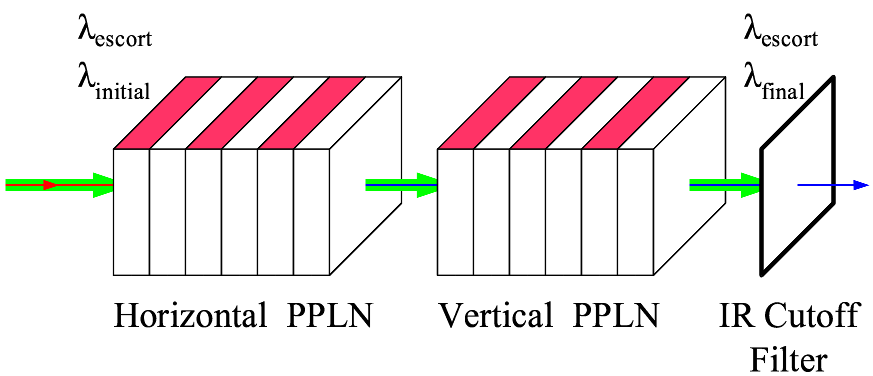

Figure 7: An arbitrarily polarized initial photon and an escort laser polarized at 45° are sent into two samples of PPLN, which respectively up-convert the H and V components of the initial photon. After the escort photons are filtered out, and the phase between the H and V components is corrected, we are left with a single high-frequency photon whose polarization state matches that of the initial photon.